

Magnetic field characteristics from HTS quadruple magnet of in-flight separator for a heavy ion accelerator

Zhan Zhang^a, Sangjin Lee^{*a}, Hyun Chul Jo^b, Do Gyun Kim^b, and Jongwon Kim^b

^a Uiduk University, Gyeongju, Korea

^b Rare Isotope Science Project, Institute for Basic Science, Korea

(Received 10 August 2015; revised or reviewed 22 September 2015; accepted 23 September 2015)

Abstract

Quadruple magnet is an essential component for the accelerator, and the field uniformity in the good field region reflects the quality of quadruple magnet. In this paper, the total magnetic field B was separated into the coil-induced magnetic field B_s and the iron-induced magnetic field B_c to explain why the total magnetic field B has some inhomogeneity. Using Fourier analysis, harmonic components of B_s , B_c and B have been analyzed at good field region, respectively. The harmonics of multipole magnet and Fourier analysis are helpful to show the uniformity of magnetic field. Several geometries of yoke and coils were defined to analyze the effect on field uniformity of an HTS quadruple magnet. By the analysis, it was found that the sixth harmonics which is the main factor of field inhomogeneity can be reduced to zero. It means that the sixth harmonics of the magnetic field B can be removed by adjusting the geometry of the magnet pole and the position of coils. We expect that this result can effectively improve the uniformity of an HTS quadruple magnet.

Keywords: field uniformity, Fourier analysis, heavy ion accelerator, HTS quadruple magnet

1. INTRODUCTION

Quadruple magnets are widely used in accelerator for focusing the transporting beams of particles [1, 2] and the field uniformity in good field region reflects the quality of the quadruple magnet. However the requirements for the field quality in the good field region of quadruple magnet can be different between applications. This study is related with the HTS quadruple magnet of RAON system from RISP(Rare Isotope Science Project) in Korea.

In order to provide the desired field configuration in quadruple magnet, appropriate position of the coils and the shape of the iron pole should be decided with high accuracy. To improve the field quality, A. Kalimov et al optimized the pole shape of quadruple magnets to remove the high-order harmonics with some preconditions [3, 4]. On the contrary, the characteristics of the magnetic field from HTS quadruple magnet was illustrated to explain the cause of inhomogeneity of quadruple magnet through this study.

Based on the HTS quadruple magnet of RAON system, the total magnetic field B was separated into the coil-induced magnetic field B_s and the iron-induced magnetic field B_c to explain why the total magnetic field B has some inhomogeneity. Using Fourier analysis, the harmonic components of B_s , B_c and B were analyzed in the good field region, respectively. In order to obtain B_s and B_c , the iron core model and air core model were established. The harmonic components of B_s were obtained in the air core model. The harmonic components of B were obtained

in the iron core model. Then, the harmonic components of B_c can be obtained from harmonic components of B_s and B .

2. THEORY

To describe the magnetic field distribution in good field region of quadruple magnet, it is convenient to express the magnetic field in terms of harmonics. The radial and the azimuthal components of magnetic flux density in polar coordinate system can be expressed as follows [5]

$$B_\rho(\rho, \varphi) = \sum_{n=1}^{\infty} K_n \rho^{n-1} \sin(n\varphi)$$
$$B_\varphi(\rho, \varphi) = \sum_{n=1}^{\infty} K_n \rho^{n-1} \cos(n\varphi)$$
(1)

where ρ is radius and φ is azimuthal angle in polar coordinate system, n is integer greater than zero, K_n are constants and B_ρ and B_φ are the radial and the azimuthal components of magnetic flux density, respectively.

If we define the amplitudes of n^{th} magnetic field component as $B_{\rho n}$ and $B_{\varphi n}$, they can be expressed by

$$B_{\rho n} = K_n \rho^{n-1}$$
$$B_{\varphi n} = K_n \rho^{n-1}$$
(2)

$B_{\rho n}$ and $B_{\varphi n}$ are constants if the radius ρ is fixed and must be same theoretically. Considering B_ρ and B_φ are periodic functions, Fourier analysis can be used to calculate $B_{\rho n}$ and $B_{\varphi n}$ like (3).

* Corresponding author: sjlee@uu.ac.kr

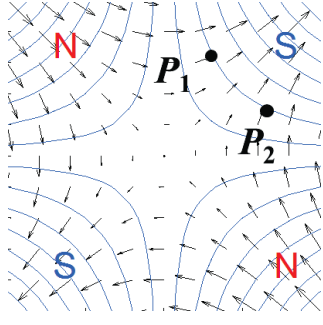


Fig. 1. Magnetic field distribution and equipotential lines for an ideal quadrupole magnet.

$$\begin{aligned} B_{\rho n} &= \frac{1}{\pi} \int_0^{2\pi} B_{\rho} \sin(n\varphi) d\varphi \\ B_{\varphi n} &= \frac{1}{\pi} \int_0^{2\pi} B_{\varphi} \cos(n\varphi) d\varphi \end{aligned} \quad (3)$$

For ideal quadrupole magnet, there is only second component i.e. 2φ component and other components are zero. Thus, we can get the magnetic flux density $B(\rho, \varphi) = \sqrt{B_{\rho}^2 + B_{\varphi}^2} = K_2 \rho = B_{\rho 2}$, therefore the magnetic field for ideal quadrupole magnet must be proportional to ρ and constant everywhere for fixed ρ . Fig. 1 shows the magnetic field distribution and the equipotential lines for an ideal quadrupole magnet. Because of symmetry, the magnetic flux density at point P_1 and point P_2 should be equal.

However some of other harmonic components inevitably exist for practical magnet. To explain the magnetic field characteristics for quadrupole magnet, we analyzed only radial component because the amplitude of radial components $B_{\rho n}$ and the amplitude of azimuthal components $B_{\varphi n}$ are same. By symmetry, the magnetic flux density can be expressed as follows

$$B_{\rho}(\rho, \varphi) = B_{\rho} \left(\rho, \frac{\pi}{2} - \varphi \right) \quad (4)$$

Using this symmetry, magnetic flux density can be expressed more recognizably like (5)

$$\begin{aligned} B_{\rho}(\rho, \varphi) &= B_{\rho 2} \sin(2\varphi) + B_{\rho 6} \sin(6\varphi) \\ &+ B_{\rho 10} \sin(10\varphi) + B_{\rho 14} \sin(14\varphi) + \dots \end{aligned} \quad (5)$$

Therefore the magnetic field in a practical quadrupole magnet has the values when $n=2, 6, 10, \dots$ and so on. 2φ component is the main value for magnetic field and 6φ or higher order components make inhomogeneity. Generally, we can define field uniformity U for quadrupole magnet as follows, because 6φ component is the main factor of field inhomogeneity. All the harmonic components were calculated for $\rho=R_{ref}$ through this paper, where R_{ref} is the reference radius for good field region.

$$U = \frac{B_{\rho 6}}{B_{\rho 2}} \times 100\% \quad (6)$$

Considering the longitudinal direction i.e. z axis, the field uniformity can be expressed even though the equation for B_{ρ} is different from (1) or (3) to express the field uniformity in the focusing area

$$\int U dz = \left(\int_{-\infty}^{+\infty} B_{\rho 6}(z) dz / \int_{-\infty}^{+\infty} B_{\rho 2}(z) dz \right) \times 100\% \quad (7)$$

The field gradient G which shows the actual maximum operating magnetic flux density of quadrupole magnet at reference radius of good field region is defined as

$$G = \frac{B_{\rho 2}}{R_{ref}} \quad (8)$$

Finally, the effective length L_{eff} [6] which means the actual length of focusing area is expressed by

$$L_{eff} = \frac{\int_{-\infty}^{+\infty} B_{\rho 2}(z) dz}{B_{\rho 2}(z=0)} \quad (9)$$

3. ANALYSIS

3.1. HTS Quadrupole Magnet

HTS quadrupole magnet is composed of an iron yoke and coils. The iron yoke is defined in Fig. 2(a), and the corresponding parameters are shown in Table I. The pole surface has hyperbolic section which is cut by a cutting line with cutting angle α . The coil was defined in Fig. 2(b), and the corresponding parameters are shown in Table II. The coil was constructed with 4 DPC HTS coils.

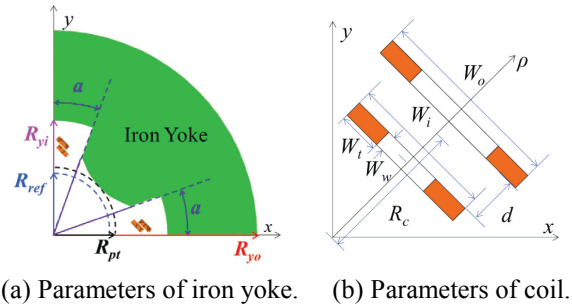


Fig. 2. Parameters for HTS quadrupole magnet.

TABLE I
PARAMETERS OF IRON YOKE.

Item	Symbol	Value
Inner radius of yoke (mm)	R_{yi}	290
Outer radius of yoke (mm)	R_{yo}	520
Yoke length (mm)	L_y	480
Pole tip radius (mm)	R_{pt}	168
Reference radius of good field region (mm)	R_{ref}	150
Angle of cutting pole ($^{\circ}$)	α	20

TABLE II
PARAMETERS OF COIL.

Item	Symbol	Value
Number of turns	N	164
Winding thickness (mm)	W_t	36.08
Winding width (mm)	W_w	12
Radius of coil (mm)	R_c	173.83
Width of inner winding (mm)	W_i	306.16
Width of outer winding (mm)	W_o	334.16
Length of coil (mm)	L_c	680.16
Gap of windings (mm)	d	2

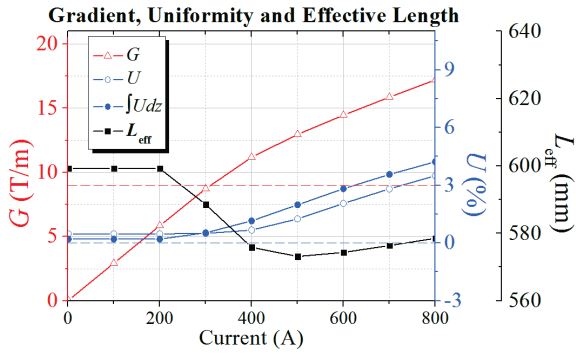


Fig. 3. Characteristics of the HTS quadruple magnet.

The electromagnetic analysis model was constructed and analyzed by MagNet™ program with the parameters of Table I and Table II. By the symmetry of analysis model, 1/16 model was established to save time in simulation.

The characteristics of the HTS quadruple magnet are shown in Fig. 3. This magnet of RAON system will be operated under the condition of $G \leq 9$ T/m and $\int U dz \leq 0.5\%$. For this condition the maximum operating current will be about 310 A and the effective length L_{eff} of this magnet can be decided greater than 587 mm.

3.2. Separation of the fields

For further analysis, the total magnetic field B was separated into the coil-induced magnetic field B_s and the iron-induced magnetic field B_c . The total magnetic flux density B inside the good field region of an HTS quadruple magnet can be separated by B_s and B_c as follows

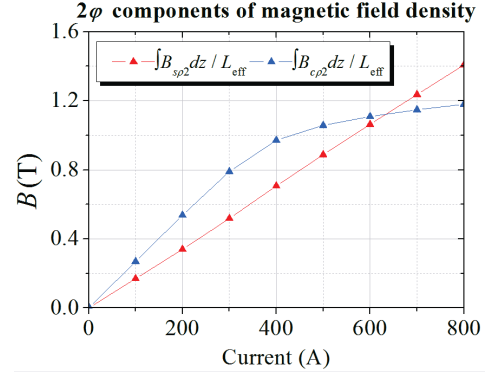
$$B = B_s + B_c \quad (10)$$

Therefore (10) will be changed to (11) for n^{th} radial component $B_{\rho n}$ of magnetic flux density.

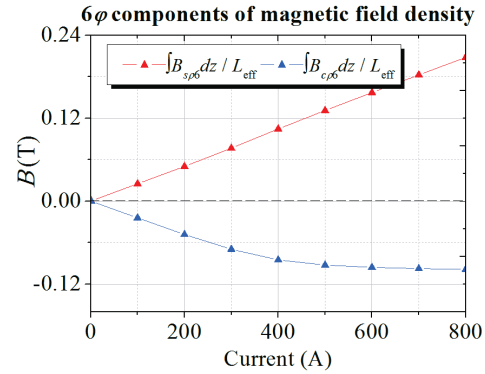
$$B_{\rho n} = B_{s\rho n} + B_{c\rho n} \quad (11)$$

where $B_{s\rho n}$ is the n^{th} radial component induced by the coil and $B_{c\rho n}$ is the n^{th} radial component induced by the core.

Because $B_{\rho n}$ was already decided and $B_{s\rho n}$ can be obtained from the air-core model i.e. the model eliminated iron yoke from Fig. 2, $B_{c\rho n}$ is easily calculated by (11). The separated field components are represented in Fig. 4. In Fig. 4, $\int B_{s\rho n} dz$ means $\int_{-\infty}^{\infty} B_{s\rho n} dz$ and



(a) 2ϕ components induced by the coil and the core.



(b) 6ϕ components induced by the coil and the core.

Fig. 4. Separated magnetic field components at the good field region of HTS quadruple magnet.

$\int B_{s\rho n} dz / L_{\text{eff}}$ is the effective or averaged magnetic field components through the magnet in longitudinal direction.

In this graph, straight lines show coil induced field B_s and saturated curves mean core induced field B_c . Fig. 4(a) explains that the 2ϕ component of magnetic flux density from the iron yoke is greater than that from the coil when the operating current is less than about 630A. And after that the 2ϕ component of magnetic flux density from the coil exceed of that from the yoke. In addition, 2ϕ components of magnetic flux density induced by the coil and the iron yoke have same sign, on the contrary 6ϕ components have opposite signs. If we can change the magnitude of each 6ϕ component, the uniformity of HTS quadruple magnet might be controlled.

3.3. Effect with respect to pole shape

In order to check the effect with respect to pole shape on the separated field components, pole tip radius R_{pt} was changed to 160, 168 and 173 mm, and cutting angle α was varied to 16° , 20° and 24° . The results are represented in Fig. 5.

In Fig. 5, $B_{s\rho 2}$ and $B_{s\rho 6}$ are not changed since the position of coils is fixed, however $B_{c\rho 2}$ and $B_{c\rho 6}$ are varied by changing the pole tip radius R_{pt} and the cutting angle α in the range of operating current. From the Fig. 5, we know that the signs of 2ϕ components and 6ϕ components are maintained by changing R_{pt} and α i.e. the signs of $B_{s\rho 2}$ and $B_{c\rho 2}$ are always same and the signs

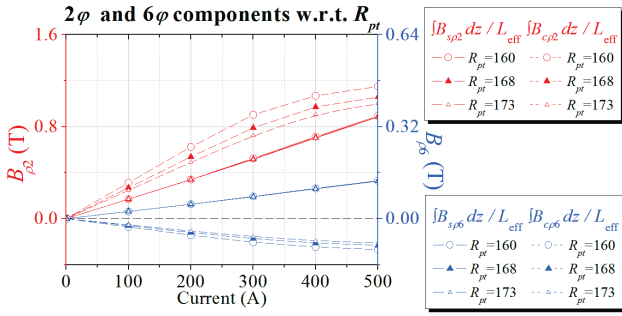
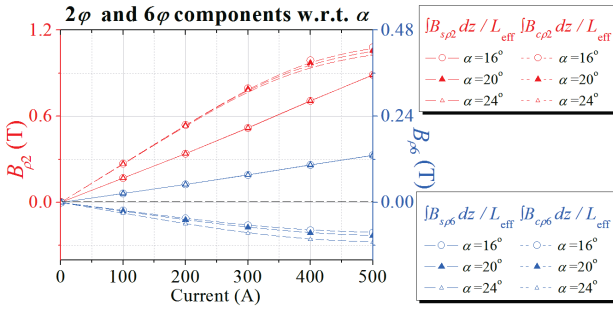
(a) Results with respect to pole tip radius R_{pt} .(b) Results with respect to cutting angle α .

Fig. 5. Effect with respect to pole shape.

of B_{sp6} and B_{cp6} are always opposite. Besides if the pole tip radius R_{pt} and the cutting angle α is decreased, which means the amount of iron pole is increased, then the magnitude of 2ϕ component from the yoke $|B_{cp2}|$ is increased. On the other hand, the amplitude of 6ϕ component from the yoke $|B_{cp6}|$ is increased when R_{pt} is decreased and α is increased. This means that the 6ϕ component from the yoke is related with the shape of iron pole.

By changing the geometry of iron pole, B_{sp6} and B_{cp6} can be matched the amplitude and kept opposite signs with each other to improve the field uniformity under the range of operating current.

3.4. Effect with respect to coil position

The position of HTS coils was moved from the center to outer side like Fig. 6 to see the effect with respect to coil position on the separated field components. Considering their cooling structure, the position of coils can be moved by the parameter of R_c . R_c was changed as 165, 175 and 185 mm here. While width of inner winding W_i and width of outer winding W_o are dependent parameters upon R_c in Fig. 6. And the other parameters are same as Table I and Table II.

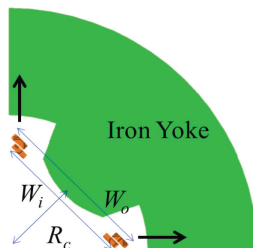


Fig. 6. Movement of coil position.

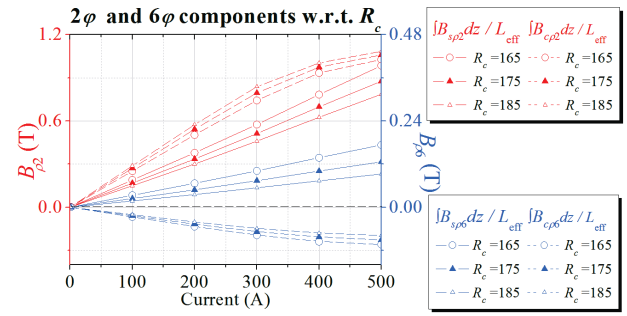


Fig. 7. Effect with respect to coil position.

The separated field components with respect to the position of coils are represented in Fig. 7. If the coil radius R_c is increased i.e. the coils are close to the iron yoke, $|B_{cp2}|$ is increased and $|B_{sp2}|$ is decreased, which means if the position of coils moves far from the center the influence of iron is increased. On the other hand, the magnitude of both 6ϕ components is decreased when R_c is increased. The effects with respect to coil position can be different with the pole shape, however the amplitude of coil induced field B_s can be changed and the signs of 2ϕ components and 6ϕ components are maintained by changing the position of coils.

4. CONCLUSION

This paper deals with the magnetic field characteristics of HTS quadruple magnet for accelerator. The total magnetic field B was separated into the coil induced magnetic field B_s and the material induced magnetic field B_c for analysis.

The signs of 2ϕ components, B_{s2} and B_{c2} , are always same, while those of 6ϕ components, B_{s6} and B_{c6} , always have opposite signs. In addition, the 2ϕ components of magnetic field are much affected with the amount of pole tip and the coil position. On the contrary, the 6ϕ components are mainly affected by the geometry of pole shape as well as the coil position. More than all, we expect the 6ϕ component of magnetic flux density which is the main factor for field inhomogeneity can be controlled by matching B_{s6} and B_{c6} for any kind of pole shape of HTS quadruple magnet. The uniformity of an HTS quadruple magnet can be effectively improved in this way.

ACKNOWLEDGMENT

This work was supported by the Rare Isotope Science Project funded by the Ministry of Science, ICT and Future Planning (MSIP) and the National Research Foundation (NRF) of Korea.

REFERENCES

- [1] Liesbeth Vanherpe, Olivier Crettiez, Alexey Vorozhtsov and Thomas Zickler, "Quadrupole Electro-magnets for Linac4 at CERN," *ATS Seminar*, Boston, 2013.

- [2] Ramesh Gupta, "Superconducting Magnets for Particle Accelerators," RISP, IBS, Korea, 2012.
- [3] A. Kalimov, P. Nalimov, "Pole Shape Optimization in Multipole Magnet," *Recent Advances in Mathematical Methods in Applied Sciences*, pp.358, 2014.
- [4] A. Kalimov, P. Nalimov, "Optimization of the Pole Shape of Quadrupole Magnets by MULTIMAG," *IEEE Trans. App. Supercond.*, vol. 16, pp.1282, 2006.
- [5] Andy Wolski, "Maxwell's Equations for Magnets--Part II: Realistic Fields," CAS Specialized Course on Magnets, Bruges, Belgium, pp.34, 2009.
- [6] J. J. Muray, "Effective Length Measurement for Quadrupole Magnets," SLAC-TN-63-010, 1963.